

See discussions, stats, and author profiles for this publication at: <https://www.researchgate.net/publication/266149472>

# Photosensitive hole transport in Schottky-contacted Si nanomembranes

Article in *Applied Physics Letters* · September 2014

DOI: 10.1063/1.4896490

CITATIONS

3

READS

43

4 authors, including:



**Ping Feng**

Nanjing University

51 PUBLICATIONS 1,095 CITATIONS

[SEE PROFILE](#)



**Guodong Wu**

Chinese Academy of Sciences

36 PUBLICATIONS 209 CITATIONS

[SEE PROFILE](#)



**Oliver G Schmidt**

Leibniz Institute for Solid State and Materials...

962 PUBLICATIONS 22,725 CITATIONS

[SEE PROFILE](#)

Some of the authors of this publication are also working on these related projects:



DFG-1156 [View project](#)



Neuromorphic Transistors for Neuromorphic Systems [View project](#)

All content following this page was uploaded by [Ping Feng](#) on 08 March 2015.

The user has requested enhancement of the downloaded file.

## Photosensitive hole transport in Schottky-contacted Si nanomembranes

Ping Feng, Guodong Wu, Oliver G. Schmidt, and Yongfeng Mei

Citation: [Applied Physics Letters](#) **105**, 121101 (2014); doi: 10.1063/1.4896490

View online: <http://dx.doi.org/10.1063/1.4896490>

View Table of Contents: <http://scitation.aip.org/content/aip/journal/apl/105/12?ver=pdfcov>

Published by the [AIP Publishing](#)

---

### Articles you may be interested in

[Reduction of the thermal conductivity in free-standing silicon nano-membranes investigated by non-invasive Raman thermometry](#)

*APL Mat.* **2**, 012113 (2014); 10.1063/1.4861796

[Optical and carrier transport properties of graphene oxide based crystalline-Si/organic Schottky junction solar cells](#)

*J. Appl. Phys.* **114**, 234506 (2013); 10.1063/1.4847515

[Single-crystal silicon/silicon dioxide multilayer heterostructures based on nanomembrane transfer](#)

*Appl. Phys. Lett.* **90**, 183107 (2007); 10.1063/1.2734367

[Stability improvement of deuterated amorphous silicon thin-film transistors characterized by modified Schottky-contact gated-four-probe method](#)

*J. Vac. Sci. Technol. B* **21**, 677 (2003); 10.1116/1.1545752

[Visible light-emitting devices with Schottky contacts on an ultrathin amorphous silicon layer containing silicon nanocrystals](#)

*Appl. Phys. Lett.* **74**, 308 (1999); 10.1063/1.123007

---



**ZABER**

Automate your set-up with  
Miniature Linear Actuators

Affordable. Built-in controllers.  
Easy to set up. Simple to use.

[www.zaber.com](http://www.zaber.com)



## Photosensitive hole transport in Schottky-contacted Si nanomembranes

Ping Feng,<sup>1,a)</sup> Guodong Wu,<sup>1</sup> Oliver G. Schmidt,<sup>2</sup> and Yongfeng Mei<sup>3,b)</sup>

<sup>1</sup>Jiangsu Provincial Key Laboratory of Photonic and Electronic Materials, School of Electronic Science and Engineering, Nanjing University, Nanjing 210093, China

<sup>2</sup>Institute for Integrative Nanosciences, IFW Dresden, Helmholtzstr. 20, Dresden D-01069, Germany

<sup>3</sup>Department of Materials Science, Fudan University, Shanghai 200433, China

(Received 25 August 2014; accepted 10 September 2014; published online 22 September 2014)

When Schottky-contacted Si nanomembranes (SiNMs; 27 nm in thickness) are exposed to light it is mainly the hole transport responding sensitively to the illumination. The electron transport on the contrary remains rather unaffected by the exposure, which cannot be explained by a simple creation of electron-hole pairs. We attribute this effect to the holes activated from SiNM surfaces, which strongly supports the existence of surface doping in SiNMs [P. P. Zhang, E. Tevaarwerk, B. N. Park, D. E. Savage, G. K. Celler, I. Knezevic, P. G. Evans, M. A. Eriksson, and M. G. Lagally, *Nature* **439**, 703–706 (2006)]. Our work suggests that the surfaces play a decisive role when creating and designing optoelectronic devices based on SiNMs. © 2014 AIP Publishing LLC.

[<http://dx.doi.org/10.1063/1.4896490>]

Silicon nanomembranes (SiNMs), for example, realized by silicon-on-insulator (SOI) technology, have shown great promise in a variety of applications such as flexible and stretchable electronics and optoelectronics,<sup>1–4</sup> radio frequency thin-film transistors,<sup>5,6</sup> and as the base to create identical Si nanowires for chemical and bio-sensors.<sup>7–9</sup> By repeated thermal oxidizing and HF etching, the thickness of SiNMs can be reduced down to less than 30 nm.<sup>10</sup> Upon thinning, the surfaces of SiNMs become more prominent to affect their physical properties.<sup>11</sup> These SiNMs have been found to possess unique electronic and thermal properties such as persistent photoconductivity,<sup>12</sup> inverse transconductance,<sup>13</sup> and remarkably reduced thermal conductivity.<sup>14–16</sup> The electrical conductance is highly sensitive to the surface of SiNMs, while the contribution from the bulk is much less pronounced.<sup>17</sup> The interaction of surface or interface energy levels with the bulk band structure enable new conduction mechanisms in SiNMs.<sup>17,18</sup> Therefore, it is important to investigate how the electron and hole transport are affected by the SiNM surfaces, which, however, have seldom been reported in previous works. Due to the presence of blocking barriers, in Schottky-contacted transistors, electrons or holes can be selected to account for the transport by tuning the gate voltage.<sup>19,20</sup> Here, we find that in Schottky-contacted SiNMs, enhanced photoresponse is observed only when holes are the dominant transport carriers. In the case of electron-dominated transport, almost no noticeable photoresponse is detected. Such an interesting effect cannot be understood by a simple creation of electron-hole pairs. We attribute it to the activation of holes from SiNM surfaces by light exposure, which thus results in the photosensitive hole transport behavior.

Schottky-contacted SiNM devices were fabricated from SOI wafers with Si/SiO<sub>2</sub> thickness of 27/100 nm (from SOITEC). The top SiNMs, doped by boron around 10<sup>15</sup> cm<sup>-3</sup> and with a resistivity of about 10 Ω cm, were patterned by photolithography and reactive ion etching. Pairs of Cr/Au

electrodes (2/30 nm) were deposited by electron beam evaporation masked with photoresist. Electrical contacts were improved through rapid thermal annealing at 500 °C for 3 min. The back Si substrate with a resistivity of about 15 Ω cm served as the gate electrode. The geometry of SiNMs as electrical channels is defined by a length and width of about 10 μm. The light source with an intensity of ~5.2 mW/cm<sup>2</sup> was provided by a normal white fluorescent lamp. The measurements were carried out by using a semiconductor parameter analyzer (Agilent 4156C). During the measurements, a bias voltage V<sub>B</sub> was applied on one electrode, while another electrode was grounded. A gate voltage V<sub>G</sub> was used to tune the carrier concentration in our SiNM channel.

In metal-semiconductor-metal (MSM) devices fabricated using lightly doped SiNMs, Schottky contacts are formed.<sup>21</sup> This is supported by analyzing the energy level alignments and indicated by the ambipolar transport characteristics. Boron-doped Si with a resistivity of 10 Ω cm corresponds to a doping level N<sub>A</sub> of about 10<sup>15</sup> cm<sup>-3</sup>. At 300 K, the intrinsic carrier concentration n<sub>i</sub> of Si is approximately 10<sup>10</sup> cm<sup>-3</sup>.<sup>22</sup> In this nondegenerate case, the separation between the Fermi level E<sub>F</sub> and the intrinsic level E<sub>i</sub> can be estimated by E<sub>F</sub> – E<sub>i</sub> = –k<sub>B</sub>T × ln(N<sub>A</sub>/n<sub>i</sub>) ≈ –0.3 eV, where k<sub>B</sub> is the Boltzmann constant and T is the temperature.<sup>22</sup> The band gap and electron affinity of single-crystalline Si are 1.12 and 4.05 eV, respectively.<sup>22</sup> The work function of Au is 4.83 eV.<sup>23</sup> Accordingly, Schottky contacts will form between the SiNM and Au. The MSM devices in this study can be viewed as two back-to-back Schottky diodes connected with a controllable Si resistor. Furthermore, note that the SiNM channel has a length of about 10 μm and a thickness of about 27 nm, so that the bias voltage at one contact has a minor effect on the Schottky barrier at the other contact. Based on this analysis, a schematic energy level alignment of the SiNM devices is shown in Fig. 1(a). Two Schottky barriers form at the contacts, with a higher barrier for electrons than holes.

Due to the high Schottky barriers, the carrier injection from the contacts mainly affects the channel current. When V<sub>B</sub> < 0, the energy levels at the contact D move upwards, as

<sup>a)</sup>Electronic mail: fengping81@gmail.com

<sup>b)</sup>Electronic mail: yfm@fudan.edu.cn

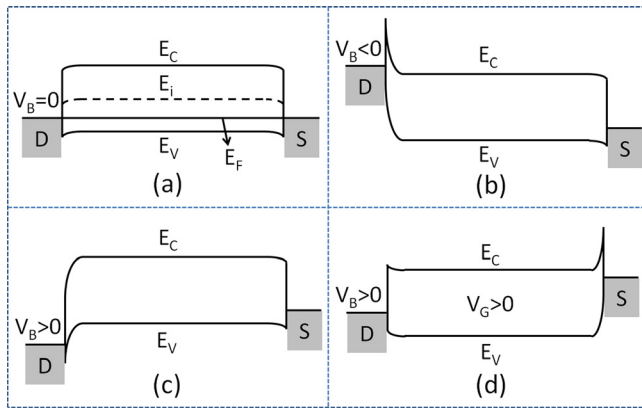


FIG. 1. Schematically drawn band diagram of the Schottky-contacted SiNM devices.  $V_B$  is applied on one electrode (D), while another electrode (S) is grounded. (a)  $V_B = 0$ , (b)  $V_B < 0$ , and (c)  $V_B > 0$  when the gate is grounded. (d) A gate modulated case at  $V_G > 0$  that is corresponding to (c), with increasing  $V_G$ , the injection of holes from D becomes difficult and the injection of electrons from S becomes much easier.  $E_C$ ,  $E_V$ ,  $E_i$ , and  $E_F$  are the conduction band, valence band, neutrality, and Fermi level of the SiNMs, respectively.

shown in Fig. 1(b), electron injection becomes much easier while hole injection from the grounded contact on the right is nearly unaffected. When  $V_B > 0$ , the energy levels at D move downwards, as shown in Fig. 1(c), hole injection is much easier. By using the gate voltage  $V_G$ , the carriers are selected to be holes or electrons. The injection of carriers from the source contact is insensitive to  $V_B$  and mainly controlled by  $V_G$ . A case for positive  $V_B$  and  $V_G$  is shown in Fig. 1(d). A transition from hole to electron transport is expected with increasing  $V_G$ . Initially, hole injection determines the channel current because electron injection from the grounded contact on the right side is difficult due to the high Schottky barrier. When increasing  $V_G$ , the hole concentration in the SiNM decreases, therefore, the current decreases gradually. With further increase in  $V_G$ , the electron concentration in the SiNM channel increases a lot and the thickness of the Schottky barrier at the grounded contact decreases, resulting in much easier injection of electrons. The main injection mechanism of electrons from the grounded contact is changed from thermionic over the Schottky barrier to tunneling through the Schottky barrier, especially at higher  $V_G$ .

The above analysis is supported by the transfer characteristics of the SiNM devices. As shown in Fig. 2(a), at a fixed  $V_B$  of 6 V and a positive  $V_G$ , with increasing  $V_G$ , the hole concentration in the SiNM channel decreased and the current decreased gradually. In this situation, electron injection from the grounded contact was difficult and its contribution to the current could be neglected. However, with further increase in  $V_G$ , as discussed in Fig. 1(d), the injection of electrons became easier due to an increased tunneling probability originating from the tuning of the Schottky barrier by  $V_G$ . As expected, a clear change-over from hole- to electron-dominated transport was observed. After this transition, the current increased with increasing  $V_G$  because injection of electrons was much easier and the electron concentration in the channel increased. Upon light exposure, the photocurrent exhibited a similar behavior. However, it can be seen that, in

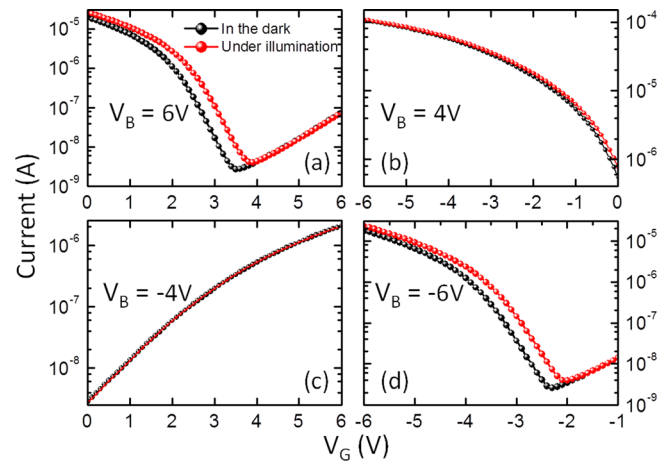


FIG. 2. Typical transfer characteristics of the Schottky-contacted SiNM devices. (a) At a fixed  $V_B$  of 6 V and positive  $V_G$ , the current versus  $V_G$  curves recorded in the dark and under illumination. A clear change-over from hole- to electron-dominated transport was observed. In the hole-dominated case, the photocurrent was higher than the dark current; in contrast, in the electron-dominated case, the photocurrent was nearly the same as the dark current. (b) At  $V_B$  of 4 V and negative  $V_G$ , holes were accumulated in the channel and injected from D. The photocurrent increased from the dark current. (c) At  $V_B$  of -4 V and positive  $V_G$ , electrons were accumulated in the channel and injected from D. The photocurrent and dark current were nearly the same. (d) At  $V_B$  of -6 V and negative  $V_G$ , the carrier transport properties were similar to that in (a). Only hole transport was sensitive to light.

the hole-dominated case, the photocurrent was higher than the dark current; in contrast, in the electron-dominated case, the photocurrent was nearly the same as the dark current.

This particular phenomenon was also observed under other voltage conditions. At a positive  $V_B$  of 4 V and negative  $V_G$ , holes were accumulated and the current was dominated by hole transport. The photocurrent was higher than the dark current, as shown in Fig. 2(b). At a negative  $V_B$  of -4 V and a positive  $V_G$ , electrons were accumulated and the current was dominated by electron transport. The photocurrent and dark current were nearly the same, as shown in Fig. 2(c). The higher Schottky barrier for electrons than holes is supported by the higher current in Fig. 2(b) than Fig. 2(c). At  $V_B = -4$  V and  $V_G = 0$ , the current was 2.88 nA; in contrast, at  $V_B = 4$  V and  $V_G = 0$ , the current was 0.55  $\mu$ A, more than two orders of magnitude higher due to a lower Schottky barrier. At a negative  $V_B$  of -6 V and negative  $V_G$ , as shown in Fig. 2(d), the carrier transport properties were similar to that in Fig. 2(a), the transition from electron- to hole-dominated transport was observed with changing  $V_G$ ; and after this transition the current was sensitive to light. Beside the typical ambipolar transport behavior, it could be seen that, only in the case of hole-dominated transport, the SiNM devices were evidently sensitive to light.

Figure 3 shows typical transfer characteristics of the SiNM devices at positive  $V_B$  and  $V_G$  by changing  $V_B$ . Along the arrow direction  $V_B$  was changed from 4 to 8 V at a step of 0.5 V. In all these curves, clear change-over from hole- to electron-dominated transport was observed, similar to that discussed in Fig. 2(a). The photocurrent was larger than the dark current only when hole transport was dominant. In electron-dominated transport, the currents were nearly the same because the injection of electrons from the grounded contact was controlled by  $V_G$  and insensitive to  $V_B$ .

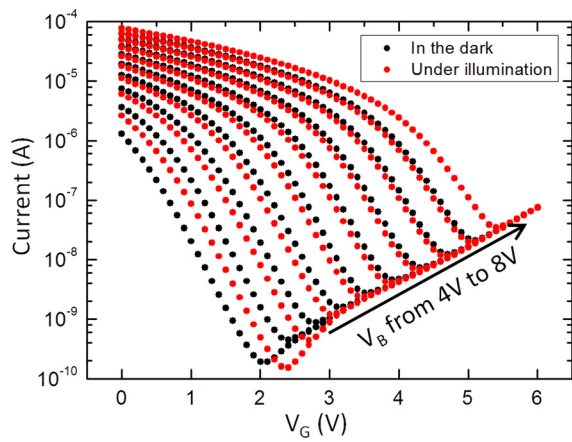


FIG. 3. Typical transfer characteristics of the SiNM devices at positive  $V_B$  and  $V_G$ . The current against  $V_G$  curves were recorded in the dark and under illumination. Along the arrow direction,  $V_B$  was changed from 4 to 8 V at a step of 0.5 V. Clear switches from hole- to electron-dominated transport were observed. The photocurrent was larger than the dark current only when hole transport was dominant. In the electron-dominated transport regions, the currents were nearly the same because electron injection from the source contact was controlled by  $V_G$  and insensitive to  $V_B$ .

The SiNM devices have two Schottky contacts; hence, the transport is mainly controlled by one type of carriers when changing  $V_B$  and  $V_G$ , as discussed above. To understand the observed unusual effects, the creation of electron-hole pairs is considered first. As a single-crystalline semiconductor with a bandgap of 1.12 eV, upon light illumination, excess carriers of both electrons and holes will be generated in the SiNMs,<sup>22</sup> and a photosensitive transport should be observed for both electrons and holes. However, only for hole transport are the SiNM devices evidently sensitive to light. Therefore, the observed effects cannot be explained by a simple creation of electron-hole pairs. In SiNMs, the electrical conductance was found to become responsive to the nature of the surfaces.<sup>17,18</sup> It has been reported that by introducing rough surfaces, persistent photoconductivity could be achieved in boron-doped SiNMs.<sup>12</sup> Such an effect only happened when hole transport was dominant. The suppression of hole transport was released upon illumination and was ascribed to hole-localized regions produced during the chemical roughening processes. The results indicated that surface defects on boron-doped SiNMs would severely affect hole concentrations. The SiNMs in this study were patterned by reactive ion etching. It was expected that although the SiNMs were protected by photoresist, there were still some defects on the surface of the SiNMs. These defects could serve as capturing centers for holes. The observed unusual effects could thus be attributed to the activation of holes from the SiNM surfaces by light exposure, which strongly supports the existence of surface doping in SiNMs.<sup>17</sup>

To further analyze the gate modulated photoresponsive characteristics of the SiNMs,  $S$  is defined as the photocurrent to dark current ratio. For the cases that the signs of  $V_B$  and  $V_G$  are the same,  $S$ - $V_G$  curves were obtained. For  $V_B > 0$  and  $V_G > 0$ , the appearances of the curves were similar, as shown in Fig. 4(a). At a fixed  $V_B$ ,  $S$  was at a low level first; with increasing  $V_G$ , it increased gradually to a high level; after that it decreased rapidly to a low level again with further

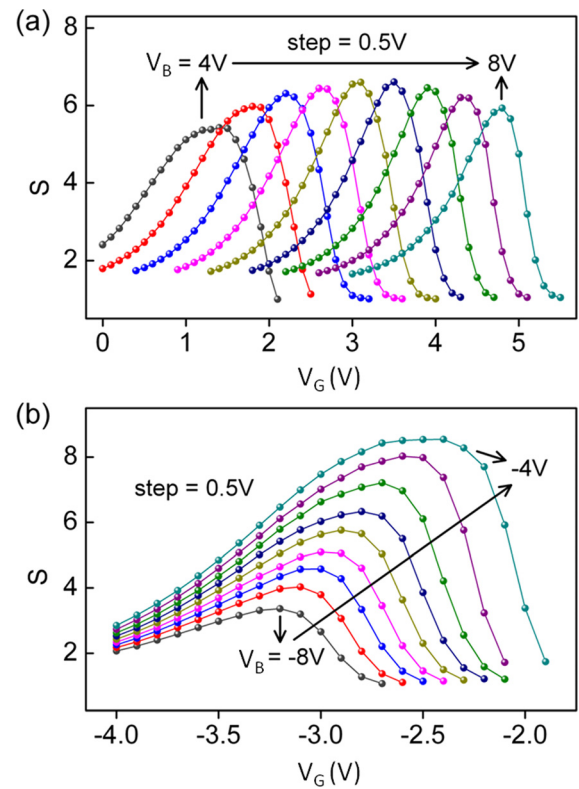


FIG. 4. The photoresponse  $S$  (photocurrent to dark current ratio) as  $V_B$  was changed (a) from 4 to 8 V and (b) from  $-8$  to  $-4$  V, respectively. The steps were 0.5 V. For positive  $V_B$ , with increasing  $V_B$ , the maximum of  $S$  ( $S_{max}$ ) shifted to higher  $V_G$ . For negative  $V_B$ , with increasing the magnitude of  $V_B$ ,  $S_{max}$  shifted to more negative  $V_G$  and decreased gradually.

increase in  $V_G$ . With increasing  $V_B$  from 4 to 8 V at a step of 0.5 V, the corresponding  $S$ - $V_G$  profiles shifted smoothly to higher  $V_G$  direction. This could be ascribed to two reasons. First, electron injection from the grounded contact was controlled by  $V_G$  and insensitive to  $V_B$ . Second, at higher  $V_B$ , hole injection was much stronger. Therefore, the transition from hole- to electron-dominated transport happened at a higher  $V_G$  and the  $S$ - $V_G$  profiles shifted forwards smoothly against  $V_G$ . For  $V_B < 0$  and  $V_G < 0$ , as shown in Fig. 4(b), with changing  $V_B$  from  $-8$  to  $-4$  V at a step of 0.5 V, the  $S$ - $V_G$  profiles expanded gradually and the positions of  $S_{max}$  shifted to lower  $|V_G|$  direction. Here, hole injection was controlled by  $V_G$  and insensitive to  $V_B$ . In addition, it is found that, in all the cases,  $S_{max}$  appeared around the position when the dominant transport switched from one type of carriers to another.

To better understand the SiNM devices,  $S_{max}$  of the curves in Figs. 4(a) and 4(b) were collected and plotted against  $V_G$  and  $V_B$ , as shown in Fig. 5. In both cases,  $|V_B|$  increased with increasing  $|V_G|$ . However, for positive  $V_B$  and  $V_G$ ,  $|V_B|$  increased much slower with increasing  $|V_G|$ . For comparison, the slope, defined by  $\alpha = \Delta V_B / \Delta V_G$ , was used as a parameter. The estimated values were  $\alpha_+ = 1.18$  and  $\alpha_- = 5$  for positive and negative cases, respectively.  $\alpha_+$  was much smaller than  $\alpha_-$ , indicating that in the latter case the gate voltage affected the devices more intensely. This could result from the much higher barrier for the injection of electrons than holes from the Schottky contacts. In the positive voltage case, hole injection was controlled by  $V_B$  and

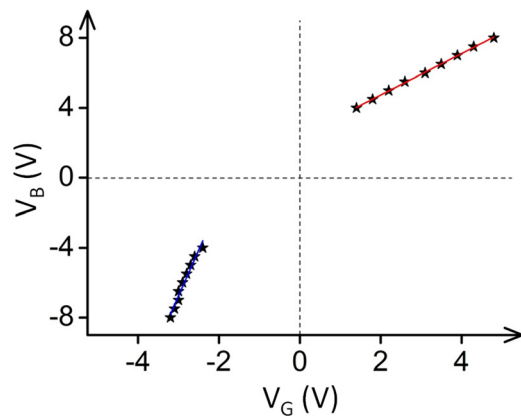


FIG. 5. Position of  $S_{max}$  in Fig. 4 plotted against  $V_G$  and  $V_B$ . In the positive voltage case (top right), the dots could be fitted to a linear curve with a slope of 1.18, while in the negative voltage case (bottom left), the dots could be fitted linearly with a slope of 5.27. These results could be understood from the higher barrier for electron injection at the Schottky contact.

electron injection by  $V_G$ . Due to the much lower barrier for hole injection, with changing  $V_B$ ,  $V_G$  would change in a much larger range to result in the transition and  $S_{max}$ . In contrast, in the negative voltage case, holes were injected from the grounded contact. Due to the much higher barrier for electron injection, with changing  $V_B$ ,  $V_G$  would change in a much smaller range for  $S_{max}$ . Therefore,  $V_G$  affected the devices more intensively when holes were injected from the grounded contact and a larger slope could be realized.

In conclusion, a photosensitive hole transport behavior was observed in Schottky-contacted SiNMs. Only when hole transport was dominant, the current across the SiNMs was sensitive to light. This unusual phenomenon could be attributed to the holes activated from the SiNM surfaces illuminated by light. The optoelectronic properties of SiNMs indicate that electrons and holes exhibit distinctive transport mechanisms and the surfaces become extremely important when building optoelectronic devices from SiNMs.

This work was supported by a Project Funded by the Priority Academic Program Development of Jiangsu Higher Education Institutions (PAPD), Specialized Research

Fund for the Doctoral Program of Higher Education (No. 20120071110025), and Science and Technology Commission of Shanghai Municipality (Nos. 12520706300 and 14JC1400200).

- <sup>1</sup>D. Y. Khang, H. Q. Jiang, Y. Huang, and J. A. Rogers, *Science* **311**, 208–212 (2006).
- <sup>2</sup>D.-H. Kim, J.-H. Ahn, W. M. Choi, H.-S. Kim, T.-H. Kim, J. Song, Y. Huang, Z. Liu, C. Lu, and J. A. Rogers, *Science* **320**, 507–511 (2008).
- <sup>3</sup>J. A. Rogers, T. Someya, and Y. Huang, *Science* **327**, 1603–1607 (2010).
- <sup>4</sup>H. Zhou, J.-H. Seo, D. M. Paskiewicz, Y. Zhu, G. K. Celler, P. M. Voyles, W. Zhou, M. G. Lagally, and Z. Ma, *Sci. Rep.* **3**, 1291 (2013).
- <sup>5</sup>G. Qin, H.-C. Yuan, G. K. Celler, J. Ma, and Z. Ma, *Appl. Phys. Lett.* **99**, 153106 (2011).
- <sup>6</sup>L. Sun, G. Qin, J.-H. Seo, G. K. Celler, W. Zhou, and Z. Ma, *Small* **6**, 2553–2557 (2010).
- <sup>7</sup>J.-H. Ahn, J. Yun, Y.-K. Choi, and I. Park, *Appl. Phys. Lett.* **104**, 013508 (2014).
- <sup>8</sup>M.-Y. Shen, B.-R. Li, and Y.-K. Li, *Biosens. Bioelectron.* **60**, 101–111 (2014).
- <sup>9</sup>E. Stern, J. F. Klemic, D. A. Routenberg, P. N. Wyrembak, D. B. Turner-Evans, A. D. Hamilton, D. A. LaVan, T. M. Fahmy, and M. A. Reed, *Nature* **445**, 519–522 (2007).
- <sup>10</sup>G. Huang and Y. Mei, *Adv. Mater.* **24**, 2517–2546 (2012).
- <sup>11</sup>P. Zhang, E. P. Nordberg, B. N. Park, G. K. Celler, I. Knezevic, P. G. Evans, M. A. Eriksson, and M. G. Lagally, *New J. Phys.* **8**, 200 (2006).
- <sup>12</sup>P. Feng, I. Mönch, S. Harazim, G. Huang, Y. Mei, and O. G. Schmidt, *Nano Lett.* **9**, 3453–3459 (2009).
- <sup>13</sup>P. Feng, I. Mönch, G. Huang, S. Harazim, E. J. Smith, Y. Mei, and O. G. Schmidt, *Adv. Mater.* **22**, 3667–3671 (2010).
- <sup>14</sup>J. Tang, H.-T. Wang, D. H. Lee, M. Fardy, Z. Huo, T. P. Russell, and P. Yang, *Nano Lett.* **10**, 4279–4283 (2010).
- <sup>15</sup>J.-K. Yu, S. Mitrovic, D. Tham, J. Varghese, and J. R. Heath, *Nat. Nanotechnol.* **5**, 718–721 (2010).
- <sup>16</sup>A. I. Boukai, Y. Bunimovich, J. Tahir-Kheli, J.-K. Yu, W. A. Goddard III, and J. R. Heath, *Nature* **451**, 168–171 (2008).
- <sup>17</sup>P. P. Zhang, E. Tevaarwerk, B. N. Park, D. E. Savage, G. K. Celler, I. Knezevic, P. G. Evans, M. A. Eriksson, and M. G. Lagally, *Nature* **439**, 703–706 (2006).
- <sup>18</sup>W. Peng, Z. Aksamija, S. A. Scott, J. J. Endres, D. E. Savage, I. Knezevic, M. A. Eriksson, and M. G. Lagally, *Nat. Commun.* **4**, 1339 (2013).
- <sup>19</sup>R. Martel, V. Derycke, C. Lavoie, J. Appenzeller, K. K. Chan, J. Tersoff, and Ph. Avouris, *Phys. Rev. Lett.* **87**, 256805 (2001).
- <sup>20</sup>G. W. Neudeck, H. F. Bare, and K. Y. Chung, *IEEE Trans. Electron Devices* **34**, 344–350 (1987).
- <sup>21</sup>S. M. Sze, D. J. Coleman, and A. Loya, *Solid-State Electron.* **14**, 1209–1218 (1971).
- <sup>22</sup>S. M. Sze and K. K. Ng, *Physics of Semiconductor Devices*, 3rd ed. (Wiley-Interscience, Hoboken, New Jersey, USA, 2006).
- <sup>23</sup>P. A. Anderson, *Phys. Rev.* **115**, 553–554 (1959).